JOC The Journal of Organic Chemistry

Article

pubs.acs.org/joc

Gas-Phase Synthesis of the Silaisocyanoethylene Molecule (C_2H_3NSi)

D. S. N. Parker, A. V. Wilson, and R. I. Kaiser*

Department of Chemistry, University of Hawai'i at Manoa, Honolulu, Hawaii 96822, United States

T. Labrador and A. M. Mebel*

Department of Chemistry and Biochemistry, Florida International University, Miami, Florida 33199, United States

Supporting Information

ABSTRACT: The gas-phase reaction between the silicon nitride radical (SiN) and the prototypical olefin—ethylene—is investigated experimentally and theoretically for the first time. Silicon nitride (SiN) and the cyano radical (CN) are isoelectronic; however, their chemical reactivities and structures are drastically different from each other. Through the use of the cross molecular beam technique, we were able to study the notoriously refractory silicon nitride radical in reaction with ethylene under single-collision conditions. We investigated the similarities and also the distinct differences with the cyano radical−ethylene system. We find that the silicon nitride radical bonds by the nitrogen atom to the double bond of ethylene; in comparison, the cyano radical adds via its carbon atom. The silicon nitride addition is barrierless, forming a long-lived $SiNCH_2CH_2$ collision complex, which is also able to isomerize via a hydrogen shift to the $SiNCHCH_3$ intermediate. Both isomers can emit a hydrogen atom via tight transition states to form the silaisocyanoethylene ($SiNC_2H_3$) molecule in an overall exoergic reaction. *This presents the very first experiment in which the silaisocyanoethylene molecule—a member of the silaisocyanide family—has been formed via a directed synthesis under gas-phase single-collision conditions.* In comparison with the isoelectronic cyano−ethylene system, the cyanoethylene (C_2H_3CN) isomer is formed. Therefore, the replacement of a single carbon atom by an isovalent silicon atom, i.e. shifting from the cyano (CN) to the silicon nitride (SiN) radical, has a dramatic influence not only on the reactivity with ethylene (carbon atom versus nitrogen atom addition) but also on the final reaction products. In the reactions of ethylene with silicon nitride and the cyano radical, the silaisonitrile over the silanitrile and the nitrile over the isonitrile reaction products are favored, respectively. This reaction provides rare experimental data for investigating the chemistry of bimolecular reactions of silicon nitride diatomics in chemical vapor deposition techniques and interstellar environments.

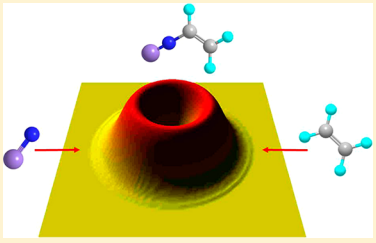

INTRODUCTION

The chemistry of silicon-bearing molecules is important in the production of semiconductors, optoelectronics, and surface growth processes such as chemical vapor disposition (CVD) and chemical etching.[1,2] In addition to these industrial applications, small silicon-carrying molecules are also chemically relevant to more "exotic" environments such as in extraterrestrial environments. Here, organosilicon molecules constitute about 10% of the molecular budget of the interstellar medium (ISM) and are of significant astronomical interest in understanding the formation of silicon−carbon-bearing dust particles.[3] The organosilicon molecules detected so far in the interstellar medium are c-SiC_2,[4] SiC,[5] SiC_4,[6] SiC_3,[7] SiCN,[8] and SiNC[9] (Figure 1).

The knowledge of the thermodynamics and reactivity of small silicon-bearing molecules is particularly important in vapor-phase epitaxy, where inaccurate control of the gas content can lead to defective materials.[10] In the production of electronically distinct silicon compounds obtainable by molecular beam epitaxy, the process can be modeled and defect layer formation can be minimized.[11] Despite the growing need for accurate experimental data on reactions of small silicon compounds, there have been only a few reports comparing the chemistry of silicon with isovalent group 14 members—namely carbon. Whereas the cyano radical (CN; $X^2\Sigma^+$) and its reactions with hydrocarbons have received considerable attention,[12] reactions of the isoelectronic silicon nitride radical (SiN; $X^2\Sigma^+$) have eluded such experimental scrutiny. Here, the generation of silicon-bearing diatomic molecules such as silicon

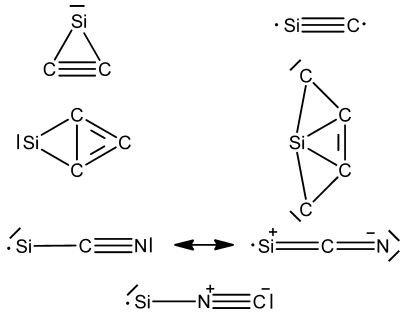

Figure 1. Classical valence structures of organosilicon molecules detected in the interstellar medium.

Received: July 20, 2012
Published: September 6, 2012

   dx.doi.org/10.1021/jo3015402 | J. Org. Chem. 2012, 77, 8574−8580

nitride (SiN; $X^2\Sigma^+$), silicon carbide (SiC; $X^3\Pi$), and silicon monoxide (SiO; $X^1\Sigma^+$) for an experimental investigation of their reactions has been fraught with difficulty, mainly due to their refractory nature.[13] Generally, silicon-bearing compounds such as Si_3N_4 have great hardness, high melting points, and high thermal-shock resistance.[1] Conversely, the analogous carbon compound cyanogen (C_2N_2) is gaseous and can be easily photodissociated to generate reactant beams of fairly reactive cyano radicals (CN; $X^2\Sigma^+$) with high intensity.[14] Silicon is known to form multiple single bonds, resulting in large structures such as silicates and Si_3N_4, while carbon compounds form multiple bonds to form small discrete molecules such as carbon dioxide (CO_2) and C_2N_2. These tendencies can be attributed to silicon having large diffuse p orbitals, coupled with a large radius of 1.46 Å in comparison to carbon's small radius of 0.91 Å and smaller, denser bonding orbitals.

With respect to the cyano radical, reactions with hydrocarbons such as acetylene (C_2H_2),[15] ethylene (C_2H_4),[16] methylacetylene (CH_3CCH),[17] allene (H_2CCCH_2),[17] propene ($H_2CCH(CH_3)$),[17] dimethylacetylene (CH_3CCCH_3),[18] and benzene (C_6H_6)[19] have been probed experimentally and theoretically to unravel the underlying reaction mechanisms and the nature of the final reaction products together with their thermodynamic properties (enthalpies of formation). These reactions were conducted under single-collision conditions in the gas phase utilizing a crossed molecular beams machine:[20] i.e., experimental conditions in which the outcome of a single-collision event between a cyano radical and a hydrocarbon molecule can be observed without any wall effects. In these reactions, the cyano radical was found to add without entrance barrier with the radical center located at the carbon atom to the sterically least hindered carbon atom of the hydrocarbon molecule C_xH_y, yielding a doublet radical intermediate of the molecular formula $[C_xH_yCN]^*$. The latter was found to undergo mainly unimolecular decomposition via atomic hydrogen loss through tight exit transition states, ultimately yielding organic nitriles (RCN; $C_xH_{y-1}CN$) such as cyanoacetylene (HCCCN), vinyl cyanide (C_2H_3CN), and cyanobenzene (C_6H_5CN) in overall exoergic reactions (eq 1).[12] No evidence

$$CN + C_xH_y \rightarrow [C_xH_yCN]^* \rightarrow C_xH_{y-1}CN + H \quad (1)$$

of any isonitrile (RNC; $C_xH_{y-1}NC$) product could be found (eq 2). Nevertheless, there have been studies of the

$$CN + C_xH_y \rightarrow [C_xH_yCN]^* \rightarrow C_xH_{y-1}NC + H \quad (2)$$

isoelectronic silicon nitride reactions, which could synthesize the hitherto elusive silanitriles (RSiN) and/or silaisonitriles (RNSi) (eqs 3 and 4, respectively).

$$SiN + C_xH_y \rightarrow [C_xH_ySiN]^* \rightarrow C_xH_{y-1}SiN + H \quad (3)$$

$$SiN + C_xH_y \rightarrow [C_xH_ySiN]^* \rightarrow C_xH_{y-1}NSi + H \quad (4)$$

Here, we present the very first crossed molecular beam study of the reaction of the isoelectronic silicon nitride radical (SiN; $X^2\Sigma^+$), with ethylene (C_2H_4) as the simplest representative of an olefinic reactant molecule and investigate the potential formation of silacyanoethylene (C_2H_3SiN) and/or silaisocyanoethylene (C_2H_3NSi). By deriving the underlying reaction dynamics and the reaction mechanism(s), this not only helps to gain a systematic understanding of the formation of small silicon-bearing molecules relevant to CVD processes and possibly to the chemistry in the interstellar medium but also assists to conduct organic radical reactions (here, radical substitution reactions of the silicon nitride radical) on the most fundamental, microscopic level. Further, studies of this kind will untangle the hitherto poorly understood chemical reactivity of small silicon-bearing radicals and assist to rationalize concepts in the chemical bonding and molecular structure of isoelectronic carbon- and silicon-bearing molecules, which are difficult to synthesize by "classical" organic methods, thus establishing the differences and similarities between these isoelectronic systems and the formation of *nitriles* (RCN) versus isonitriles (RNC) and silanitriles (RSiN) versus silaisonitriles (RNSi).

RESULTS

Experimental Results. Reactive scattering signals were recorded at a mass to charge ratio (m/z) of 69. This finding alone demonstrates that, in the reaction of the silicon nitride radical with ethylene, a molecule with the molecular formula of $^{28}SiNC_2H_3$ is formed via the silicon nitride−atomic hydrogen exchange pathway. Further, we should stress that no reactive scattering signal of a molecular hydrogen loss yielding the $^{28}SiNC_2H_2$ species (m/z 68) was observed, indicating that the molecular hydrogen loss channel is closed under our experimental conditions. It is worth noting that according to our calculations the $SiNC_2H_2^+$ cation is a stable species, which can exist in at least two isomeric forms, $SiNCCH_2^+$ (C_{2v}, $^1A_1$) and cyclic c-$SiNC_2H_2^+$ (C_{2v}, $^1A_1$) (see the Supporting Information for optimized geometries and molecular parameters), with the former being 178 kJ mol^{-1} lower in energy than the latter. For instance, the energies required for the fragmentation of $SiNCCH_2^+$ to $SiNCCH^+$ + H, SiN^+ + C_2H_2, and SiN + $C_2H_2^+$ are computed to be as high as 426, 609, and 722 kJ mol^{-1}, respectively. The calculated adiabatic ionization energies of potential $^{28}SiNC_2H_2$ products, $SiNC_2H_2$ to form c-$SiNC_2H_2^+$ and $SiNCCH_2$ to form $SiNCCH_2^+$, are 7.59 and 6.87 eV, respectively, and thus ionization of $^{28}SiNC_2H_2$ should be possible with our ionizer operating at 80 eV. Also, no signal was observed at the adduct peak of m/z 70 ($^{28}SiNC_2H_4$) or any other ($^{28}SiNC_2H_4$) fragments. On the basis of the previous experimental experience, we anticipate that the ionization cross section will not vary by orders of magnitude between the possible $SiNC_2H_x$ species, and therefore if present such species should be detectable in our experiment. To conclude, the analysis of the raw data alone indicates that the only observable product corresponds to a molecule with the formula $^{28}SiNC_2H_3$. The time-of-flight spectra obtained for the product at m/z 68 for different laboratory angles could be integrated to derive the laboratory angular distribution (Figure 2). It should be noted that the main aim of measuring the intensity of the mass spectrum for the $SiNC_2H_3$ molecule at m/z 68 is to obtain the relative intensity of the $SiNC_2H_3$ molecule at different angles in the angular distribution and the time the $SiNC_2H_3$ molecule takes to reach the detector. The time-of-flight spectra give us information on the translational energy from the formation of the product, i.e. thermodynamic information, where short TOF times imply a high reaction exoergicity. Here, mass spectroscopy is used as a filter to measure the relative

dx.doi.org/10.1021/jo3015402 | J. Org. Chem. 2012, 77, 8574−8580

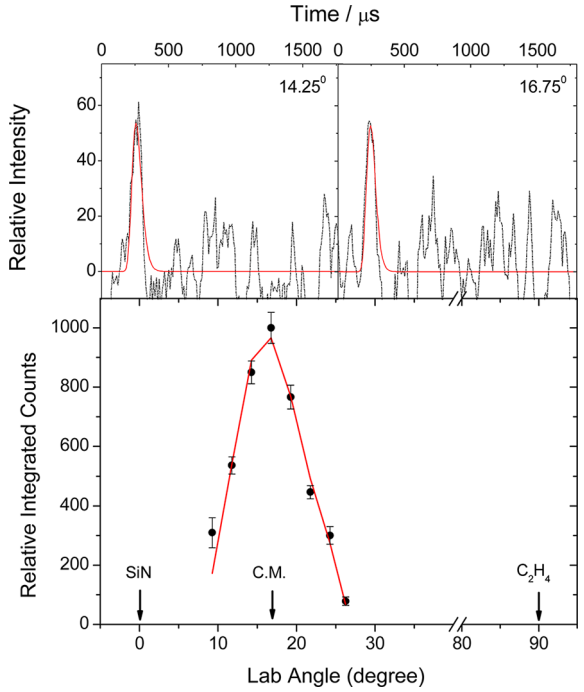

Figure 2. (bottom) Laboratory angular distribution at m/z 69 of the ionized C_2H_3NSi product from the reaction of the silicon nitride radical with ethylene. The direction of the silicon nitride radical beam is defined as 0° and that of the ethylene beam as 90°. The solid line represents the angular distribution obtained from the best-fit center-of-mass angular and translational energy distributions, and the black squares represent the experimental data. (top) Time-of-flight spectra recorded at 14.25 and 16.75°. The black dash-dotted line represents the experimental data and the solid red line the best fit from the center-of-mass functions.

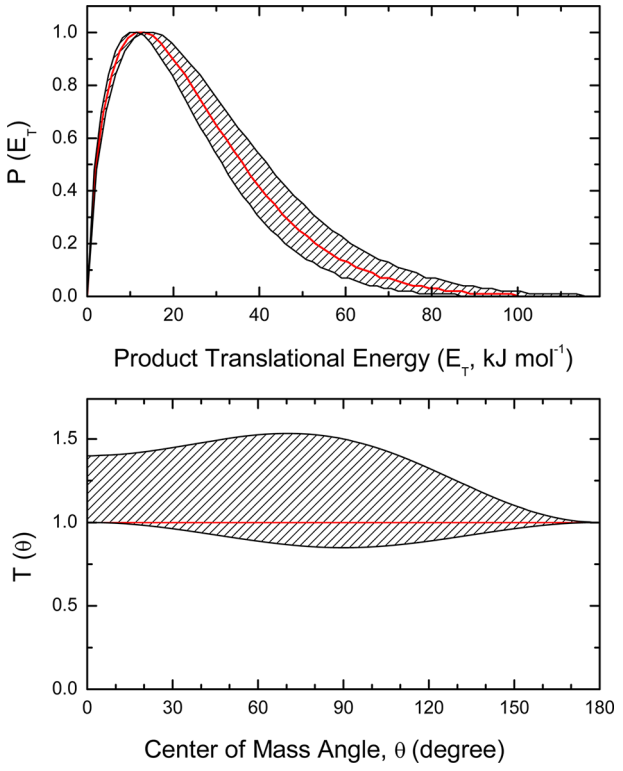

Figure 3. Center-of-mass translational energy distribution (top) and center-of-mass angular distribution (bottom) for the reaction of silicon nitride (SiN; $X^2\Sigma^+$) with ethylene (C_2H_4; X^1A_g) to form the silaisocyanoethylene molecule (C_2H_3NSi) plus atomic hydrogen at a collision energy of 35.9 ± 3.5 kJ mol^{-1}. The solid red lines represent the "best fits", and the hatched areas represent the error limits to the fits.

intensities of a particular product formed in a gas-phase reaction at different angles and times. The refractory nature of the reaction and therefore the low signal of the products mean a traditional mass spectrum spanning a range of masses is an unfeasible measurement to take, as well not being relevant to the analysis using the crossed molecular beam approach.

The laboratory angular distribution is relatively narrow, extends by only about 20° in the scattering plane defined by the primary and secondary beams, and depicts a pronounced maximum close to the center-of-mass (CM) angle of 17.2 ± 1.2°; these observations suggest that the reaction likely proceeds via indirect (complex forming) scattering dynamics involving $^{28}SiNC_2H_4$ reaction intermediate(s). Finally, it should be stressed that both sets of laboratory data (TOF spectra, laboratory angular distribution) could be fit with a single channel with the mass combination of 69 amu ($^{28}SiNC_2H_3^+$) plus 1 amu (H) utilizing the center of mass functions shown in Figure 3.

By analyzing these center-of-mass functions, we obtain crucial information on the chemical dynamics of the system. Since the TOF spectra verified the formation of $^{28}SiNC_2H_3$ isomer(s), we shall first attempt to unravel the nature of the reaction product. The center-of-mass translational energy distribution, $P(E_T)$, depicts a maximum translational energy release of 100 ± 20 kJ mol^{-1}. From the conservation of energy, we can calculate the reaction exoergicity by subtracting the collision energy of 35.9 ± 3.5 kJ mol^{-1} from the maximum energy released. Here, we see that the reaction forming the $^{28}SiNC_2H_3$ isomer(s) plus atomic hydrogen is exoergic by 64 ± 24 kJ mol^{-1}. Also, the flux distribution peaks away from zero translational energy at about 8−14 kJ mol^{-1}; this finding indicates that at least one reaction channel to form the $^{28}SiNC_2H_3$ isomer(s) plus hydrogen has a tight exit transition state (repulsive bond rupture involving a significant electron rearrangement from the decomposing intermediate to the final products).[21] In other words, the reversed reaction of a hydrogen atom addition to the $^{28}SiNC_2H_3$ product has an entrance barrier of this magnitude.[22] Finally, the center-of-mass translational energy distribution also allows us to determine the average energy released into the translational degrees of freedom of the products to be 25 ± 8 kJ mol^{-1}: i.e., about 25% of the total available internal energy. This order of magnitude is also consistent with the reaction proceeding through indirect scattering dynamics.[23]

The center-of-mass angular distribution, $T(\theta)$, as shown in Figure 3 possesses additional important features to constrain the reaction mechanism. First, the center-of-mass angular distribution depicts intensity over the complete range from 0 to 180°; this finding indicates that the reaction dynamics are indirect and involve the formation of $^{28}SiNC_2H_4$ intermediate(s), before the latter decomposes via atomic hydrogen elimination to the $^{28}SiNC_2H_3$ product(s).[21] In detail, the "best fit" presents an isotropic distribution (flat), indicating that the lifetime of the complex is longer than its rotational period and that the coupling between the initial and final orbital angular momentum is weak (poor polarization); in other words, there is no preferential emission direction of the light hydrogen atom loss.[21] However, within the error limits of the fits, we can

dx.doi.org/10.1021/jo3015402 | J. Org. Chem. 2012, 77, 8574−8580

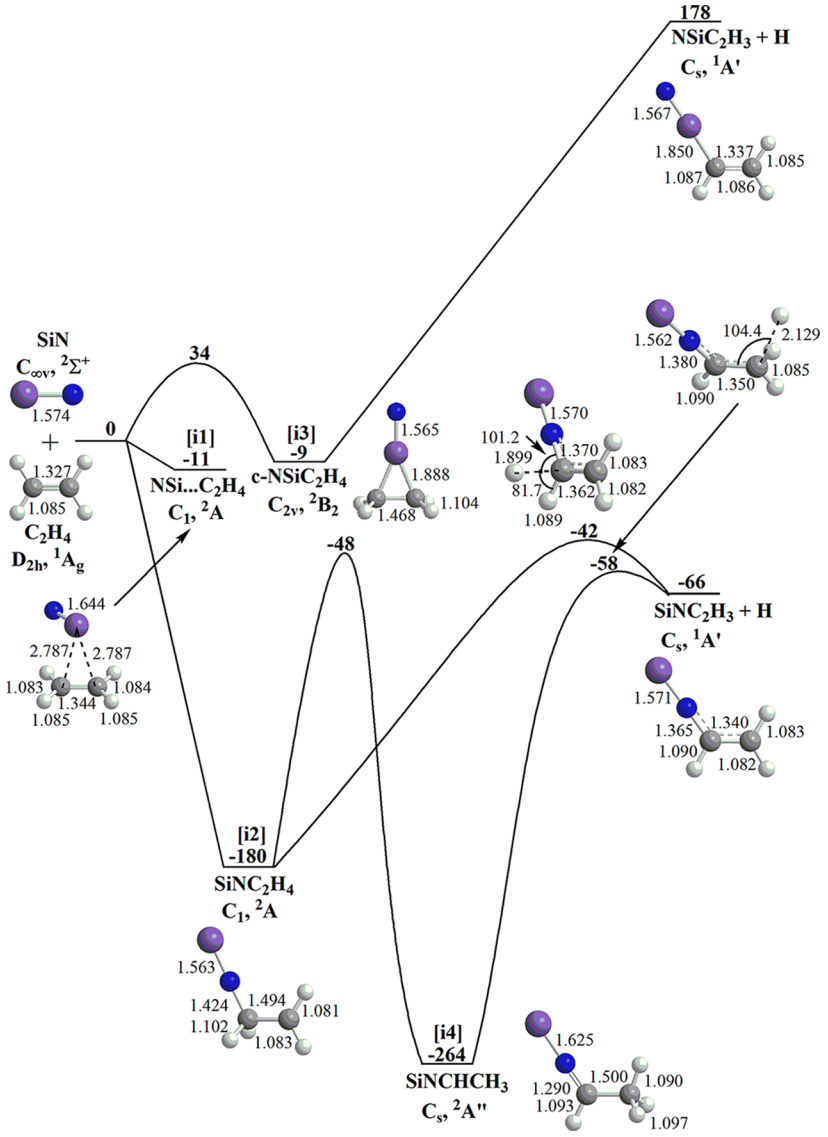

Figure 4. Schematic representation of the $SiNC_2H_4$ potential energy surface. Energies calculated at the CCSD(T)/CBS//B3LYP/6-311G** level are shown in kJ mol^{-1} and are relative to the silicon nitride plus ethylene reactants. Bond lengths are given in Å and bond angles are in deg (see the Supporting Information for detailed geometric structures of all species involved in the reaction and their rotational constants and vibrational frequencies).

obtain a reasonable fit of the laboratory data with a slight forward scattering with respect to the silicon nitride beam: i.e., a ratio of the intensity at the poles, $I(180°)/I(0°)$, of 0.72 ± 0.38. This slight forward scattering is indicative of a collision complex with lifetimes comparable to its rotational period, i.e. of about 1.4 times the rotational period, in line with the osculating complex model.[24] Further, within the error limits of the fits, the center-of-mass angular distribution depicts a slight peak at θ = 70°, suggesting geometrical constraints when the decomposing complex emits a hydrogen atom: i.e., a preferential hydrogen loss parallel to the total angular momentum vector and almost perpendicular to the rotational plane of the decomposing complex.

Theoretical Results. To complement the information gained experimentally, the reaction of silicon nitride with the ethylene molecule was also investigated computationally. Figure 4 compiles the doublet $^{28}SiNC_2H_4$ potential energy surface (PES) accessed in the reaction of the silicon nitride radical with ethylene. The computations suggest that the reaction can proceed via three entrance channels: (i) formation of the weakly bound (−11 kJ mol^{-1}) van der Waals complex [i1], (ii) addition of the silicon nitride radical with its nitrogen atom to one carbon atom of the ethylene molecule, yielding intermediate [i2], which resides in a deep potential energy well of −180 kJ mol^{-1} with respect to the separated reactants, and (iii) addition of the silicon nitride radical with the silicon atom to the π electron density of ethylene to form a cyclic intermediate, c-$NSiC_2H_4$ ([i3]), which is only slightly more stable than the separated reactants by 9 kJ mol^{-1}. Note that only the pathway leading to the cyclic intermediate was found to have an entrance barrier of about 34 kJ mol^{-1}; the remaining pathways are barrierless. We carefully searched for any isomerization pathways of the van der Waals complex [i1] to any $^{28}SiNC_2H_4$ isomer but were not successful. Therefore, even if formed, all van der Waals complexes dissociate back to the separated reactants under single-collision conditions in the gas phase. It is worth mentioning that intermediate [i3] can decompose to the silacyanoethylene product plus atomic

dx.doi.org/10.1021/jo3015402 | J. Org. Chem. 2012, 77, 8574−8580

hydrogen (C_2H_3SiN). However, the overall reaction is endoergic by 178 kJ mol^{-1}. This endoergicity cannot be compensated for by our collision energy of only 35.9 ± 3.5 kJ mol^{-1}; therefore, even intermediate [i3] can only undergo unimolecular decomposition back to the silicon nitride and ethylene reactants. In summary, although three entrance channels exist, only the addition of the silicon nitride radical with its nitrogen atom to the ethylene molecule yielding intermediate [i2] presents an open pathway. In terms of chemical bonding, [i2] can be described as |Si═N−CH_2−$C^{\bullet}H_2$.

What is the fate of this collision complex? Our calculations suggest two pathways are available. First, intermediate [i2] can undergo a hydrogen loss, yielding the silaisocyanoethylene isomer plus atomic hydrogen (C_2H_3NSi) through a tight exit transition state located about 24 kJ mol^{-1} above the separated products. The overall reaction energy to form silaisocyanoethylene plus atomic hydrogen was computed to be 66 kJ mol^{-1}, and the bonding in this molecule is expressed as |Si═N—CH═CH_2.

An alternate pathway also exists from the initial intermediate [i2]. Here, a barrier of 132 kJ mol^{-1} must be overcome, which is associated with a hydrogen migration from the central to the terminal carbon atom in [i2] to reach the global potential energy minimum of the $^{28}SiNC_2H_4$ potential energy surface: the $SiNCHCH_3$ intermediate [i4], which is bound by 264 kJ mol^{-1} and can be described as a |Si═N−$C^{\bullet}$H−CH_3 ↔ |$Si^{\bullet}$−N═CH−CH_3 resonance. From here, intermediate [i4] can emit a hydrogen atom to also yield the silaisocyanoethylene isomer; a tight exit transition state and an 8 kJ mol^{-1} exit barrier are associated with this pathway. Here, the exit barrier refers to the energy of the transition state relative to the products and can be thought as an entrance energy barrier in the reversed addition of hydrogen atom to the product ($SiNCHCH_2$). It should be noted that no molecular hydrogen loss pathways from [i2] or [i4] have been found; a search of saddle points for H_2 elimination converged to the H atom loss transition states.

DISCUSSION

We are combining now the experimental and computational results in an attempt to extract the underlying mechanism of the reaction of the silicon nitride radical with ethylene. First, let us derive the nature of the $SiNC_2H_3$ reaction product. The center-of-mass translational energy distribution, $P(E_T)$, shows a reaction exoergicity of 64 ± 24 kJ mol^{-1}, which correlates nicely with the computationally derived reaction exoergicity of 66 kJ mol^{-1} to form the silaisocyanoethylene isomer (C_2H_3NSi). Recall that, considering the collision energy of only 35.9 ± 3.5 kJ mol^{-1}, the reaction yielding the silacyanoethylene isomer (C_2H_3SiN) plus atomic hydrogen is too endoergic to be open. Having identified the silaisocyanoethylene isomer (C_2H_3NSi) as the sole reaction product, we now compare the molecular structures of the reactants with the final product to derive the reaction mechanism. Since in the silaisocyanoethylene product (C_2H_3NSi) a nitrogen−carbon bond is formed, we have to conclude that the silicon nitride radical adds with its nitrogen atom to the ethylene molecule, yielding intermediate [i2]. This formation of the initial collision complex leads to an indirect reaction; recall that the indirect nature of the reaction mechanism was derived from the shape of the center-of-mass angular distribution. The reaction intermediate [i2] can then emit a hydrogen atom, forming the silaisocyanoethylene product (C_2H_3NSi), or isomerize via a hydrogen shift to [i4], which then undergoes unimolecular decomposition via hydrogen emission to silaisocyanoethylene (C_2H_3NSi) from the terminal methyl (CH_3) group. Both pathways are connected with tight transition states. This correlates nicely with our experimental findings, since the translational energy distribution depicts a peaking away from 0 at 8−14 kJ mol^{-1}, which in turn suggests tight exit transition state(s) upon decomposition of the $SiNC_2H_4$ intermediate(s) to silaisocyanoethylene (C_2H_3NSi) plus atomic hydrogen. Note that, within our error limits, a peaking of the center-of-mass angular distribution at θ = 70° suggests a preferential hydrogen loss almost perpendicular to the rotational plane of the decomposing complex. A comparison of this finding with the geometry of the exit transition states (Figure 4) shows that indeed the hydrogen atom leaves almost perpendicularly with respect to the plane containing the remaining C_2H_3NSi fragment. In case of the reverse reaction, the hydrogen atom approaches almost perpendicularly to the plane of the silaisocyanoethylene (C_2H_3NSi) molecule and, upon interaction with the carbon−carbon double bond, adds to the π electron density at the C1 or C2 carbon atom, leading to intermediates [i2] and [i4], respectively.

How does the reaction dynamics of the silicon nitride radical compare with that of the isoelectronic cyano radical−ethylene system? Interestingly, the cyano reaction can be initiated without entrance barrier through an addition of the *carbon atom* of the cyano radical to the carbon−carbon double bond of ethylene; no addition with the nitrogen atom of the cyano radical was found to be important. This is unlike the silicon nitride radical reaction, where the addition with the nitrogen atom is the only route open. Both addition pathways lead to reaction intermediates (NCC_2H_4 and $SiNC_2H_4$), with the NCC_2H_4 collision complex being 52 kJ mol^{-1} more stable than the $SiNC_2H_4$ intermediate, relative to their respective reactants. This difference is representative of the enhanced bond energy of the C−C single bond in comparison to the relatively weaker N−C bond. Once the initial intermediates are formed, the reaction dynamics start to show marked similarities, with both systems having two accessible pathways. The initial collision complex (XC_2H_4; X = CN, NSi) can either decompose via hydrogen loss through tight transition states, leading to XC_2H_3 (X = CN, NSi) products; alternatively, the complex XC_2H_4 (X = CN, NSi) first undergoes a hydrogen shift to $XCHCH_3$ followed then by a hydrogen emission, also via tight exit transition states. In the cyano−ethylene system, the formation of the cyanoethylene product (C_2H_3CN) is 30 kJ mol^{-1} more exoergic relative to their reactants in comparison to the thermic synthesis of the silaisocyanoethylene product (C_2H_3NSi). This difference in reaction energies can be related to bond stabilities, where a C−C bond in C_2H_3CN is more stable than the C−N bond in C_2H_3NSi.

CONCLUSION

We investigated the chemical dynamics of the reaction of the silicon nitride radical (SiN) with ethylene (C_2H_4) under single-collision conditions and also investigated this system theoretically using electronic structure calculations. Our data propose that the reaction was indirect, occurring via complex formation involving the addition of the silicon nitride radical with its nitrogen atom to the olefinic bond of the ethylene molecule. This leads to the formation of a $SiNC_2H_4$ reaction intermediate. The latter was found to undergo unimolecular decomposition via a tight exit transition state to silaisocyano-

dx.doi.org/10.1021/jo3015402 | J. Org. Chem. 2012, 77, 8574−8580

ethylene (C_2H_3NSi) plus atomic hydrogen. The overall reaction was found to be exoergic by 64 ± 24 kJ mol^{-1}. In comparison with the isoelectronic reaction of the cyano radical with ethylene, in which the cyano radical adds with the carbon atom to the olefin, the present reaction prefers addition by the nitrogen of silicon nitride radical to the ethylene bond, thus resulting in a product with a carbon−nitrogen bond rather than a carbon−carbon bond. This results in a reaction yielding silaisocyanoethylene (C_2H_3NSi) in comparison to cyanoethylene (C_2H_3CN). We hope that this protocol can be further utilized to investigate the synthesis of additional members of the poorly characterized silaisocyano family.

EXPERIMENTAL SECTION

The experiments were carried out under single-collision conditions in a crossed molecular beam instrument.[12] Briefly, a pulsed supersonic beam of ground-state silicon nitride (SiN; $X^2\Sigma^+$) was produced in situ via laser ablation of silicon, and the ablated silicon atoms were entrained in nitrous oxide carrier gas (N_2O, 99.99%) in the primary source region of the vacuum chamber. The silicon was ablated by focusing the fourth harmonic of a Nd:YAG laser operating at 1064 nm and 30 Hz onto the rod at a peak power of 20 mJ per pulse. The rotating silicon rod was mounted on a homemade ablation source that was driven by an external stepper motor.[25] The rotary motion was delivered to the mounted rod by a flexible drive shaft connected to a rotary feed through a setup which benefits from the stepper motor being outside the vacuum chamber. The nitrous oxide (N_2O) carrier gas was introduced via a pulsed valve operating at repetition rates of 60 Hz with amplitudes of −350 V and opening times of 80 μs, where it reacted with the ablated silicon atoms most likely via nitrogen abstraction to produce silicon nitride. A backing pressure of 4 atm for the nitrous oxide source resulted in a pressure of about 1×10^{-4} Torr in the primary source chamber. It was found that the number density of the silicon nitride radicals utilizing nitrous oxide carrier gas was about 1 order of magnitude larger than when operated with nitrogen gas. The molecular beam including the silicon nitride radicals passed a skimmer and a four-slot chopper wheel, which selected a segment of the pulsed silicon nitride beam of a well-defined peak velocity of v_p = 2140 ± 95 ms^{-1} and speed ratio S = 3.9 ± 1.3.

The silicon nitride beam crossed a pulsed beam of ethylene (C_2H_4) perpendicularly, released by a second pulsed valve at 550 Torr; the intersecting segment of the ethylene beam had a peak velocity of 905 ± 10 ms^{-1} and speed ratio of 9.2 ± 0.2. Assisted by two frequency dividers and three pulse generators, a photodiode mounted on top of the chopper wheel provided the time zero trigger for the experiment. The primary and secondary pulsed valves opened 1840 and 1860 μs after the time zero, as defined by the photodiode. The collision energy between the silicon nitride and ethylene molecules was 35.9 ± 3.5 kJ mol^{-1}. Silicon has three isotopes, m/z 28 (92.23%), m/z 29 (4.67%), and m/z 30 (3.1%); the reported collision energy refers to the ^{28}Si isotope.

The reaction products were monitored using a triply differentially pumped quadrupole mass spectrometer (QMS) in the time-of-flight (TOF) mode after electron-impact ionization of the neutral molecules at 80 eV with an emission current of 2 mA; up to 1.9×10^7 TOFs had to be collected at each angle. The ionized products were separated according to their mass to charge ratio by a quadrupole mass spectrometer operated with an oscillator at 2.1 MHz; only ions with the desired mass to charge (m/z) value passed through and were accelerated toward a stainless steel "door knob" target coated with an aluminum layer and operated at a voltage of −22.5 kV. The ions hit the surface and initiated an electron cascade that was accelerated by the same potential until they reached an aluminum-coated organic scintillator, whose photon cascade was detected by a photomultiplier tube (operated at −1.35 kV). The signal from the PMT was then filtered by a discriminator (1.6 mV) prior to feeding into a multichannel scaler to record time-of-flight spectra.[26,27] TOF spectra were recorded at 2.5° intervals over the angular distribution. The TOF spectra recorded at each angle and the product angular distribution in the laboratory frame (LAB) were fit using a forward-convolution routine.[28,29] This method uses an initial choice of the product translational energy $P(E_T)$ and the angular distribution $T(\theta)$ in the center-of-mass reference frame (CM) to create TOF spectra and a product angular distribution. The $P(E_T)$ and $T(\theta)$ values were iteratively optimized until the best fit was reached.

Theoretical Methods. Geometries of various species involved in the reaction were optimized at the hybrid density functional B3LYP level[30,31] with the 6-311G** basis set, and vibrational frequencies were calculated using the same B3LYP/6-311G** method. For the entrance channel leading to the initial complex [i2], the absence of the barrier was additionally verified by a search of the corresponding transition state at the quadratic configuration interaction QCISD/6-311G** level, which, similarly to the B3LYP/6-311G** calculations, led to the separated reactants. Relative energies were refined by employing the coupled cluster CCSD(T) method[32−34] with Dunning's correlation-consistent cc-pVDZ, cc-pVTZ, cc-pVQZ, and cc-pV5Z basis sets.[35] The total CCSD(T) energies were extrapolated to the complete basis set (CBS) limit by fitting the equation[36] $E_{tot}(x) = E_{tot}(\infty) + Be^{-Cx}$, where x is the cardinal number of the basis set (2, 3, 4, and 5 for cc-pVDZ, cc-pVTZ, cc-pVQZ, and cc-pV5Z, respectively) and $E_{tot}(\infty)$ is the CCSD(T)/CBS total energy. Spin-restricted coupled cluster RCCSD(T) calculations were used for open-shell structures. All ab initio and density functional calculations were performed using the GAUSSIAN-09[37] and MOLPRO 2010[38] program packages. The theoretical methods applied here have been accessed in the literature,[39] and the CCSD(T)/CBS + ZPE(B3LYP/6-311G**) relative energies are expected to be accurate within ±5 kJ mol^{-1}, whereas the B3LYP approach normally provides bond lengths and bond angles accurate within 0.01−0.02 Å and 1−2°, respectively, and vibrational frequencies within a few percent.

ASSOCIATED CONTENT

Supporting Information

A table giving optimized Cartesian coordinates, rotational constants, and vibrational frequencies of various species (reactants, intermediates, products, and transition states) involved in the SiN + C_2H_4 reaction. This material is available free of charge via the Internet at http://pubs.acs.org.

AUTHOR INFORMATION

Corresponding Author

*E-mail: ralfk@hawaii.edu (R.I.K.); mebela@fiu.edu (A.M.M.).

Notes

The authors declare no competing financial interest.

ACKNOWLEDGMENTS

This work was supported by the U.S. National Science Foundation (CHE-0948258).

REFERENCES

(1) Oyedepo, G. A.; Peterson, C.; Wilson, A. K. *J. Chem. Phys.* **2011**, *135*, 094103/1−094103/12.
(2) Sari, L.; McCarthy, M. C.; Schaefer, H. F.; Thaddeus, P. *J. Am. Chem. Soc.* **2003**, *125*, 11409−11417.
(3) MacKay, D. D. S.; Charnley, S. B. *Mon. Not. R. Astron. Soc.* **1999**, *302*, 793−800.
(4) Thaddeus, P.; Cummins, S. E.; Linke, R. A. *Astrophys. J.* **1984**, *283*, L45−L48.
(5) Cernicharo, J.; Gottlieb, C. A.; Guelin, M.; Thaddeus, P.; Vrtilek, J. M. *Astrophys. J.* **1989**, *341*, L25−L28.
(6) Ohishi, M.; Kaifu, N.; Kawaguchi, K.; Murakami, A.; Saito, S.; Yamamoto, S.; Ishikawa, S.; Fujita, Y.; Shiratori, Y.; Irvine, W. M. *Astrophys. J.* **1989**, *345*, L83−L86.
(7) Apponi, A. J.; McCarthy, M. C.; Gottlieb, C. A.; Thaddeus, P. *Astrophys. J.* **1999**, *516*, L103−L106.

(8) Guelin, M.; Muller, S.; Cernicharo, J.; Apponi, A. J.; McCarthy, M. C.; Gottlieb, C. A.; Thaddeus, P. *Astron. Astrophys.* **2000**, *363*, L9−L12.
(9) Guelin, M.; Muller, S.; Cernicharo, J.; McCarthy, M. C.; Thaddeus, P. *Astron. Astrophys.* **2004**, *426*, L49−L52.
(10) Segal, A. S.; Vorob'ev, A. N.; Karpov, S. Y.; Mokhov, E. N.; Ramm, M. G.; Ramm, M. S.; Roenkov, A. D.; Vodakov, Y. A.; Makarov, Y. N. *J. Cryst. Growth* **2000**, *208*, 431−441.
(11) Wong, H.-W.; Nieto, J. C. A.; Swihart, M. T.; Broadbelt, L. J. *J. Phys. Chem. A* **2004**, *108*, 874−897.
(12) Kaiser, R. I.; Balucani, N. *Acc. Chem. Res.* **2001**, *34*, 699−706.
(13) McCarthy, M. C.; Gottlieb, C. A.; Thaddeus, P. *Mol. Phys.* **2003**, *101*, 697−704.
(14) Black, G.; Jusinski, L. E.; Taherian, M. R.; Slanger, T. G.; Huestis, D. L. *J. Phys. Chem.* **1986**, *90*, 6842−8.
(15) Huang, L. C. L.; Asvany, O.; Chang, A. H. H.; Balucani, N.; Lin, S. H.; Lee, Y. T.; Kaiser, R. I.; Osamura, Y. *J. Chem. Phys.* **2000**, *113*, 8656−8666.
(16) Balucani, N.; Asvany, O.; Chang, A. H. H.; Lin, S. H.; Lee, Y. T.; Kaiser, R. I.; Osamura, Y. *J. Chem. Phys.* **2000**, *113*, 8643−8655.
(17) Huang, L. C. L.; Balucani, N.; Lee, Y. T.; Kaiser, R. I.; Osamura, Y. *J. Chem. Phys.* **1999**, *111*, 2857−2860.
(18) Balucani, N.; Asvany, O.; Chang, A. H. H.; Lin, S. H.; Lee, Y. T.; Kaiser, R. I.; Bettinger, H. F.; Schleyer, P. v. R.; Schaefer, H. F., III *J. Chem. Phys.* **1999**, *111*, 7472−7479.
(19) Balucani, N.; Asvany, O.; Chang, A. H. H.; Lin, S. H.; Lee, Y. T.; Kaiser, R. I.; Bettinger, H. F.; Schleyer, P. v. R.; Schaefer, H. F., III *J. Chem. Phys.* **1999**, *111*, 7457−7471.
(20) Zhang, F.; Gu, X.; Guo, Y.; Kaiser, R. I. *J. Org. Chem.* **2007**, *72*, 7597−7604.
(21) Gu, X.; Guo, Y.; Zhang, F.; Mebel, A. M.; Kaiser, R. I. *Faraday Discuss.* **2006**, *133*, 245−275.
(22) Lee, Y.-T.; McDonald, J. D.; LeBreton, P. R.; Herschbach, D. R. *Rev. Sci. Instrum.* **1969**, *40*, 1402−8.
(23) Levine, R. D. *Molecular Reaction Dynamics*; Cambridge University Press: Cambridge, U.K., 2005.
(24) Miller, W. B.; Safron, S. A.; Herschbach, D. R. *Discuss. Faraday Soc.* **1967**, *44*, 108−22.
(25) Gu, X.; Guo, Y.; Kawamura, E.; Kaiser, R. I. *J. Vac. Sci. Technol.* **2006**, *24*, 505−511.
(26) Gu, X. B.; Guo, Y.; Kawamura, E.; Kaiser, R. I. *Rev. Sci. Instrum.* **2005**, *76*, 083115/1−083115/6.
(27) Guo, Y.; Gu, X.; Kawamura, E.; Kaiser, R. I. *Rev. Sci. Instrum.* **2006**, *77*, 034701/1−034701/9.
(28) Vernon, M. Thesis, University of California, Berkeley, CA, 1981.
(29) Weis, M. S. Ph.D. Thesis, University of California, Berkeley, CA, 1986.
(30) Becke, A. D. *J. Chem. Phys.* **1993**, *98*, 5648−52.
(31) Lee, C.; Yang, W.; Parr, R. G. *Phys. Rev. B: Condens. Matter* **1988**, *37*, 785−9.
(32) Purvis, G. D., III; Bartlett, R. J. *J. Chem. Phys.* **1982**, *76*, 1910−18.
(33) Scuseria, G. E.; Janssen, C. L.; Schaefer, H. F., III *J. Chem. Phys.* **1988**, *89*, 7382−7.
(34) Scuseria, G. E.; Schaefer, H. F., III *J. Chem. Phys.* **1989**, *90*, 3700−3.
(35) Dunning, T. H., Jr. *J. Chem. Phys.* **1989**, *90*, 1007−23.
(36) Peterson, K. A.; Dunning, T. H., Jr. *J. Phys. Chem.* **1995**, *99*, 3898−901.
(37) Frisch, M. J.; Trucks, G. W.; Schlegel, H. B.; et al. *Gaussian 09, Revision A.1*; Gaussian, Inc., Wallingford, CT, 2009.
(38) MOLPRO, version 2010.1, a package of ab initio programs: Werner, H.-J.; Knowles, P. J.; Knizia, G.; Manby, F. R.; Schütz, M.; et al.; see http://www.molpro.net.
(39) Cramer, C. J. *Essentials of Computational Chemistry*; Wiley: Chichester, U.K., 2004.